Available online at www.sciencedirect.com
ScienceDirect
Procedia Engineering 90 (2014) 268 – 274
Procedia Engineering
www.elsevier.com/locate/procedia

10th International Conference on Mechanical Engineering, ICME 2013

Pressure-driven flow instability with convective heat transfer through a curved rectangular duct of small aspect ratio

Rabindra Nath Mondal[a,]* and Md. Saidul Islam[b]

[a] *Department of Mathematics, Jagannath University, Dhaka-1100, Bangladesh*
[b] *Department of Mathematics, Hamdard University, Narayangonj, Bangladesh*

Abstract

The present study investigates unsteady fluid flow through a curved rectangular duct of aspect ratio 0.5 and curvature 0.5. Numerical calculations are carried out by using a spectral method, and covering a wide range of the pressure gradient parameter, the Dean number, $6000 \le Dn \le 12000$ and the Grashof number, $100 \le Gr \le 2000$ for two cases of the duct, *Case-I:* Stationary duct and *Case-II:* Rotating duct. The outer wall of the duct is heated while the inner wall cooled. The main concern of the present study is to discuss the unsteady flow behavior *i.e* whether the unsteady flow is steady-state, periodic, multi-periodic or chaotic, if Dn or Gr is increased. For a stationary duct, we investigate the unsteady flow characteristics for the Dean number $6000 \le Dn \le 12000$ and the Grashof number $100 \le Gr \le 2000$, and it is found that the unsteady flow undergoes in the scenario '*steady-state* $\rightarrow$ *periodic* $\rightarrow$ *multi-periodic* $\rightarrow$ *chaotic*', if Gr is increased. For rotating duct, however, we investigate the unsteady flow characteristics for the Taylor number $-100 \le Tr \le 1000$, and it is found that the unsteady flow undergoes through various flow instabilities, if Dn or Gr is increased. Typical contours of secondary flow patterns and temperature profiles are also obtained, and it is found that the unsteady flow consists of a single-, two-, and multi-vortex solutions.

Selection and peer-review under responsibility of the Department of Mechanical Engineering, Bangladesh University of Engineering and Technology (BUET)

Keywords: Rotating curved rectangular duct; secondary flow; unsteady flow; Dean number; Chaos.

1. Introduction

Recently, great attention has been paid for the study of flow and heat transfer through curved ducts and channels

* Corresponding author. Tel.: +88-01710851580; Fax: +88-02-7113752.
E-mail address: rnmondal71@yahoo.com

Selection and peer-review under responsibility of the Department of Mechanical Engineering, Bangladesh University of Engineering and Technology (BUET)
doi:10.1016/j.proeng.2014.11.848

because of their ample applications in fluids engineering. Since rotating machines were introduced into engineering applications, such as rotating systems, gas turbines, electric generators, heat exchangers, cooling system and some separation processes, scientists have paid considerable attention to study rotating curved duct flows. The readers are referred to Nandakumar and Masliyah [1] and Yanase *et al.* [2] for some outstanding reviews on curved duct flows.

The fluid flowing in a rotating curved duct is subjected to two forces: the *Coriolis force* due to rotation and the *centrifugal force* due to curvature. For isothermal flows of a constant property fluid, the Coriolis force tends to produce vortices while centrifugal force is purely hydrostatic. When a temperature induced variation of fluid density occurs for non-isothermal flows, both Coriolis and centrifugal type buoyancy forces can contribute to the generation of vortices. These two effects of rotation either enhance or counteract each other in a non-linear manner depending on the direction of wall heat flux and the flow domain. Therefore, the effect of system rotation is more subtle and complicated and yields new; richer features of flow and heat transfer in general, bifurcation and stability in particular, for non-isothermal flows. Selmi and Nandakumer [3] and Yamamoto *et al*. [4] performed studies on the flow in a rotating curved rectangular duct. Recently, Mondal *et al.* [5] performed numerical prediction of the non-isothermal flows through a rotating curved square duct. They performed time-evolution calculations of the unsteady solutions with and without symmetry condition. Mondal *et al.* [6] performed numerical prediction of the unsteady solutions for rotating curved square duct flow with negative rotation and discussed the transitional behavior of the unsteady solutions. Employing finite volume method, Wang and Cheng [7] examined the flow characteristics and heat transfer in curved square ducts for positive rotation and found reverse secondary flow for the co-rotation cases. Recently, Mondal *et al.* [8] performed numerical investigation of the non-isothermal flows through a rotating curved square duct and obtained substantial results. In the succeeding paper, Mondal *et al.* [9] performed spectral numerical study to investigate the unsteady flow characteristics for the non-isothermal flows through a curved rectangular duct and showed transitional behavior of the unsteady solutions. However, there is no known study on the rotating curved rectangular duct flows for small aspect ratio. The present paper is, therefore, an attempt to fill up this gap with studying the effects of rotation on the flow characteristics for such flows.

2. Governing Equations

Consider a hydro-dynamically and thermally fully developed two-dimensional flow of viscous incompressible fluid through a rotating curved duct with rectangular cross section, whose height and wide are *2h* and *2l*, respectively. The coordinate system with the relevant notation is shown in Fig. 1. The system rotates at a constant angular velocity Ω_T around the y' axis. It is assumed that the outer wall of the duct is heated while the inner wall cooled. The variables are non-dimensionalized by using the representative length and velocity.

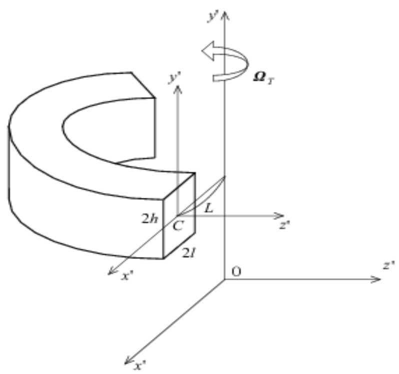

Fig. 1. Coordinate system.

Since the flow field is uniform in the z direction, the sectional stream function ψ is introduced as,

$$u = \frac{1}{1+\delta x}\frac{\partial \psi}{\partial y}, \quad v = -\frac{1}{1+\delta x}\frac{\partial \psi}{\partial x}. \tag{1}$$

The basic equations for the axial velocity *w*, the stream function ψ and the temperature T are derived from the Navier-Stokes equations and the energy equation under the *Boussinesq approximation* as,

$$(1+\delta x)\frac{\partial w}{\partial t}+\frac{2\partial(w,\psi)}{\partial(x,y)}-Dn+\frac{\delta^2 w}{1+\delta x}=(1+\delta x)\Delta_2 w-\frac{2\delta}{(1+\delta x)}\frac{\partial \psi}{\partial y}w+\delta\frac{\partial w}{\partial x}-\delta Tr\frac{\partial \psi}{\partial y} \tag{2}$$

$$\left(\Delta_2-\frac{\delta}{1+\delta x}\frac{\partial}{\partial x}\right)\frac{\partial \psi}{\partial t}=-\frac{2}{(1+\delta x)}\frac{\partial(\Delta_2\psi,\psi)}{\partial(x,y)}+\frac{2\delta}{\left(1+\delta x\right)^2}\times\left[\frac{\partial \psi}{\partial y}\left(2\Delta_2\psi-\frac{3\delta}{1+\delta x}\frac{\partial \psi}{\partial x}+\frac{\partial^2 \psi}{\partial x^2}\right)\right.$$
$$\left.-\frac{\partial \psi}{\partial x}\frac{\partial^2 \psi}{\partial x \partial y}\right]+\frac{\delta}{\left(1+\delta x\right)^2}\times\left[3\delta\frac{\partial^2 \psi}{\partial x^2}-\frac{3\delta^2}{1+\delta x}\frac{\partial \psi}{\partial x}\right]-\frac{2\delta}{1+\delta x}\frac{\partial}{\partial x}\Delta_2\psi+2w\frac{\partial w}{\partial y}+\Delta_2^2\psi$$
$$-Gr(1+\delta x)\frac{\partial T}{\partial x}+\frac{1}{2}Tr\frac{\partial w}{\partial y}, \tag{3}$$

$$\frac{\partial T}{\partial t}+\frac{1}{(1+\delta x)}\frac{\partial(T,\psi)}{\partial(x,y)}=\frac{1}{\Pr}\left(\Delta_2 T+\frac{\delta}{1+\delta x}\frac{\partial T}{\partial x}\right) \tag{4}$$

where, $\Delta_2 \equiv \frac{\partial^2}{\partial x^2}+\frac{4\partial^2}{\partial y^2}$, $\frac{\partial(f,g)}{\partial(x,y)}\equiv\frac{\partial f}{\partial x}\frac{\partial g}{\partial y}-\frac{\partial f}{\partial y}\frac{\partial g}{\partial x}$

The non-dimensional parameters Dn, the Dean number, Tr, the Taylor number, *Gr*, the Grashof number and *Pr*, the Prandtl number, which appear in equations (2) to (4) are defined as:

$$Dn=\frac{Gl^3}{\mu\upsilon}\sqrt{\frac{2l}{L}}, \quad Tr=\frac{2\sqrt{2\delta}\Omega_T l^3}{\upsilon\delta}, \quad Gr=\frac{\beta g\Delta T d^3}{\upsilon^2}, \quad \Pr=\frac{\upsilon}{\kappa} \tag{5}$$

where the parameters denote their usual meaning. In this study, the aspect ratio is considered as 0.5, *Gr* =100, $\delta = 0.5$ and $\Pr = 7.0$ (water). The rigid boundary conditions for w and ψ are used as

$$w(\pm 1,y)=w(x,\pm 1)=\psi(\pm 1,y)=\psi(x,\pm 1)=\frac{\partial \psi}{\partial x}(\pm 1,y)=\frac{\partial \psi}{\partial y}(x,\pm 1)=0 \tag{6}$$

and the temperature T is assumed to be constant on the walls as $T(1,y)=1,\quad T(-1,y)=-1,\quad T(x,\ \pm 1)=x.$

3. Method of Numerical Calculations

In order to obtain the numerical solutions, spectral method is used. The main objective of the method is to use the expansion of the polynomial functions i.e. the variables are expanded in the series of functions consisting of Chebyshev polynomials. By this method the expansion functions $\phi_n(x)$ and $\psi_n(x)$ are expressed as

$$\left.\begin{aligned}\varphi_n(x)&=(1-x^2)C_n(x),\\ \psi_n(x)&=(1-x^2)^2 C_n(x)\end{aligned}\right\} \tag{7}$$

where $C_n(x)=\cos\left(n\cos^{-1}(x)\right)$ is the *n*-th order Chebyshev polynomial. $w(x,y,t)$, $\psi(x,y,t)$ and $T(x,y,t)$ are expanded in terms of the expansion functions $\phi_n(x)$ and $\psi_n(x)$ as

$$\left.\begin{aligned} w(x,y,t) &= \sum_{m=0}^{M}\sum_{n=0}^{N} w_{mn}(t)\phi_m(x)\phi_n(y) \\ \psi(x,y,t) &= \sum_{m=0}^{M}\sum_{n=0}^{N} \psi_{mn}(t)\psi_m(x)\psi_n(y). \\ T(x,,y,t) &= \sum_{m=0}^{M}\sum_{n=0}^{N} T_{mn}\phi_m(x)\phi_n(y)+x \end{aligned}\right\} \tag{8}$$

where M and N are the truncation numbers. In order to calculate the unsteady solutions, the Crank-Nicolson and Adams-Bashforth methods together with the function expansion (8) and the collocation methods are applied.

4. Resistance Coefficient

We use the resistance coefficient λ as one of the representative quantities of the flow state. It is also called the *hydraulic resistance coefficient*, and is generally used in fluids engineering, defined as

$$\frac{P_1^* - P_2^*}{\Delta z^*} = \frac{\lambda}{dh^*}\frac{1}{2}\rho\left\langle w^*\right\rangle^2, \tag{9}$$

where quantities with an asterisk denote the dimensional ones, $\langle\,\rangle$ stands for the mean over the cross section of the rectangular duct.. Since $\left(P_1^* - P_2^*\right)/\Delta z^* = G,$ λ is related to the mean non-dimensional axial velocity $\langle w\rangle$ as

$$\lambda = \frac{16\sqrt{2\delta}Dn}{3\langle w\rangle^2}, \tag{10}$$

5. Results and Discussion

5.1 Case I: Non-Rotating Duct

We studied the time evolution of λ for $Dn = 10500$ at Gr = 1500 as shown in Figure 2(a). We found that the flow is steady-state for $Dn = 10500$ at Gr = 1500. Note that the unsteady flow for $Dn < 10500$ is also steady-state. We also show typical contours of secondary flow patterns and temperature profiles in Fig. 2(b).

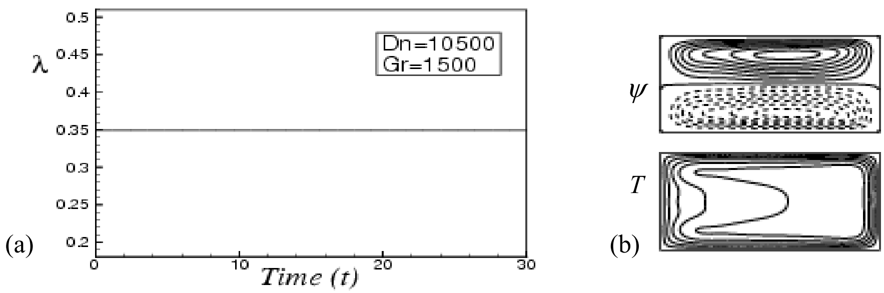

Fig. 2. (a) Time evolution of λ at time $0 \le t \le 30$ for $Dn = 10500$ and $Gr = 1500$ for the aspect ratio 0.5 and curvature 0.5; (b) Secondary flow pattern and temperature profile for $Dn = 10500$ and $Gr = 1500$.

Then, we studied the time evolution for $Dn = 11000$ at Gr =1000 as shown in Fig. 3(a). We found that the flow is multi-periodic for $Dn = 11000$ at Gr = 1000. In order to see the multi-periodic oscillations more clearly, we show contours of secondary flow patterns, temperature profiles and axial flow distribution in Fig. 3(b). It is found that the unsteady flow is an asymmetric two-vortex solution. We obtained time evolution of λ for $Dn = 12000$ at Gr =1500, it is found that the flow is chaotic for $Dn = 12000$ at Gr = 1500. In order to see the chaotic flow behavior, we also obtained typical contours of secondary flow patterns, temperature profiles and axial flow distribution, and it is found that the unsteady flow is an asymmetric two-vortex solution. The results are not shown here for brevity.

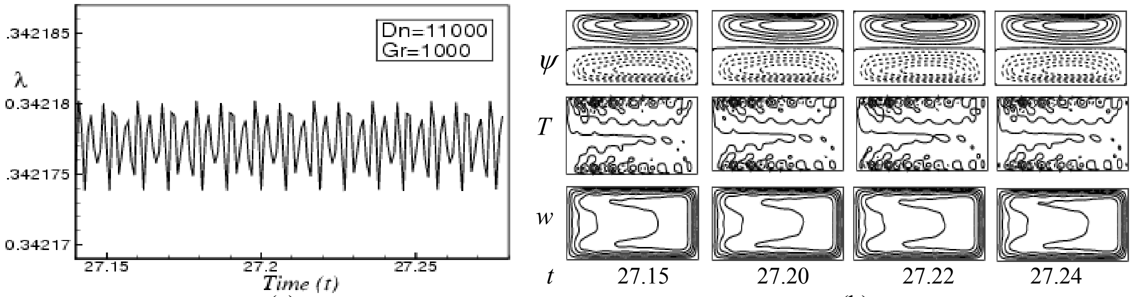

(a) (b)

Fig. 3. (a) Time evolution of λ for $Dn = 11000$ and $Gr = 1000$; (b) Secondary flow patterns (top), temperature profiles (middle) and axial flow distribution (bottom) for $Dn = 11000$ and $Gr = 1000$.

5.2 Case II: Rotating duct

We studied the time evolution of λ for the rotating curved duct at $Dn = 10750$ and Tr = -100 as shown in Fig. 4(a). It is found that the flow is a steady-state solution for $Dn = 10750$. We also show typical contours of secondary flow patterns and axial flow distribution as shown in Fig. 4(b). It is found that the secondary flow is a two-vortex solution. Then we studied the time evolution of λ for $Dn = 10750$ and Tr = - 500 as shown in Fig. 5(a). We found that the flow is periodic for $Dn = 10750$. Contours of secondary flow patterns and temperature profile are shown in Fig. 5(b). As seen in Fig. 5(b), the periodic flow oscillates between asymmetric two-vortex solutions for Tr = -100.

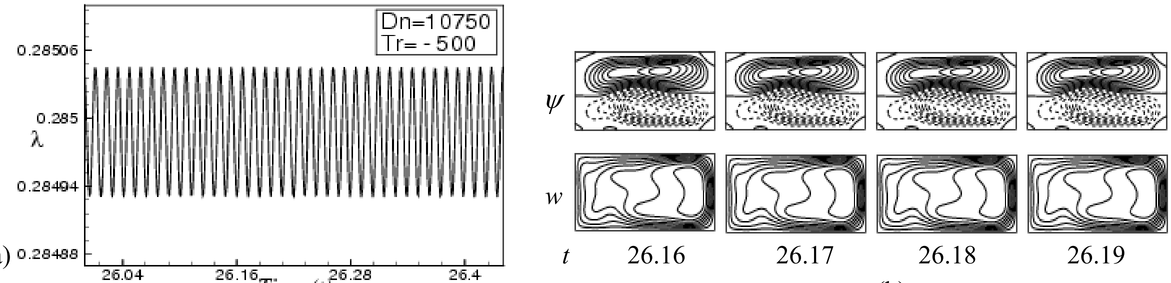

(a) (b)

Fig. 4. (a) Time evolution of λ for $Dn = 10750$ and $Tr = -500$; (b) Secondary flow patterns (top) and axial flow distribution (bottom) for $Dn = 10750$ and $Tr = -500$.

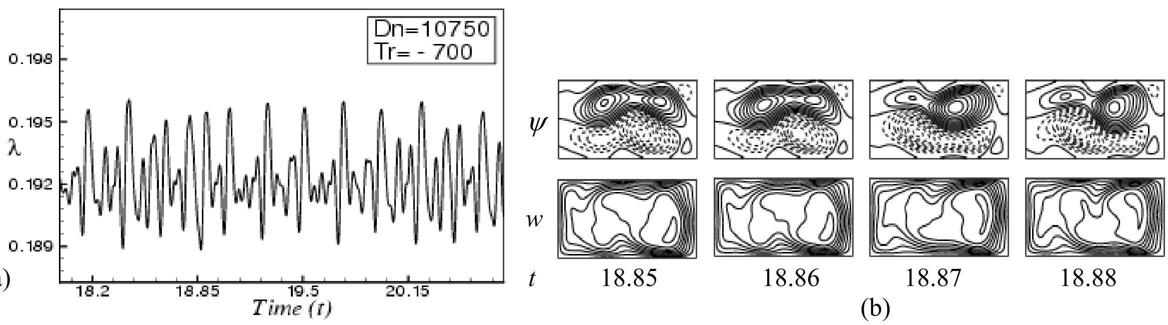

(a) (b)

Fig. 5. (a) Time evolution of λ for $Dn = 10750$ and $Tr = -700$; (b) Secondary flow patterns (top) and axial flow distribution (bottom) for $Dn = 10750$ and $Tr = -700$.

We then studied time evolution of λ for $Dn = 10750$ and Tr = - 700 as shown in Fig. 5(a). It is found that the flow is chaotic for $Dn = 10750$ and Tr = - 700. In order to view the flow behavior of chaotic solution clearly, we also show typical contours of secondary flow patterns and axial flow distribution in Fig. 5(b). As seen in Fig. 5(b), the chaotic flow oscillates between asymmetric six-vortex solutions.

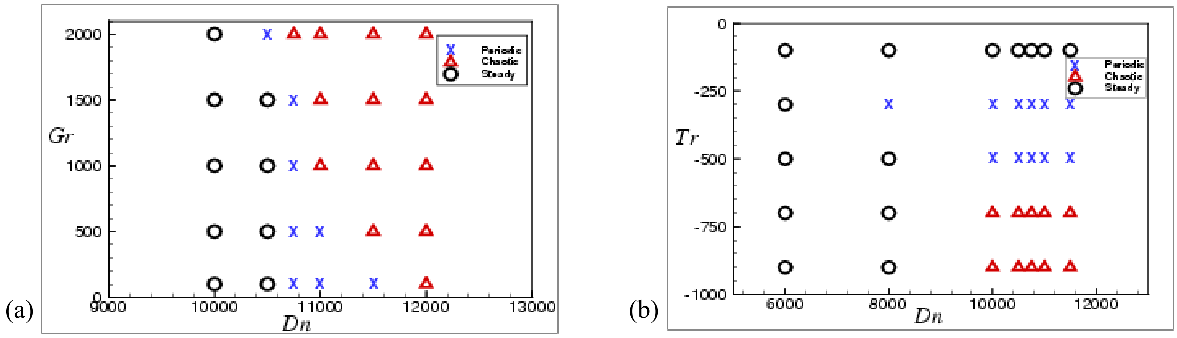

Fig. 6. Unsteady solutions at a glance aspect ratio 0.5 and curvature 0.5, (a) Non-rotating duct; (b) Rotating duct.

Phase diagrams in the $Dn - Gr$ and $Dn - Tr$ plane

Finally, we show complete unsteady solutions obtained by the numerical computation in the present study, by two phase diagrams in Fig. 6(a) in the $Dn - Gr$ and $Dn - Tr$ planes for $9000 \le Dn \le 13000$ and $0 \le Gr \le 2000$ for the stationary duct flow, while in Fig. 6(b) in the $Dn - Tr$ plane for $5000 \le Dn \le 12000$ and $-900 \le Tr \le 0$ for the rotating curved duct flow. In this figure, circles indicate steady-state solution, crosses periodic solution and triangles chaotic solution. As seen in Fig. 6, the steady flow turns into chaotic flow through periodic or multi-periodic flows.

6. Conclusion

The present study addresses fully developed two dimensional flow of viscous incompressible fluid flow through a curved rectangular duct of aspect ratio 0.5 and for strong curvature 0.5. Numerical calculations are carried out by using a spectral method, and covering a wide range of the pressure gradient parameter, the Dean number, $6000 \le Dn \le 12000$ and the Grashof number, $100 \le Gr \le 2000$ for two cases of the duct, *Case-I:* Non-Rotating duct and *Case-II:* Rotating duct. After a comprehensive survey over the parametric ranges for a stationary curved duct, it is found that the unsteady flow undergoes in the scenario '*steady-state* $\rightarrow$ *periodic* $\rightarrow$ *multi-periodic* $\rightarrow$ *chaotic*', if *Gr* is increased. For a rotating curved duct, we considered the rotation of the duct in the negative direction, and it is found that steady-state flow turns into chaotic flow through periodic or multi-periodic oscillations, if *Dn* or *Gr* is increased. Typical contours of secondary flow patterns and temperature profiles are also obtained, and it is found that the unsteady flow consists of a single-, two-, and multi-vortex solutions. It is suggested that chaotic flows enhance heat transfer more effectively in the fluid than the periodic solutions because of the formation of many secondary vortices appearing at the outer wall of the duct.

References

[1] K. Nandakumar and J. H. Masliyah, Swirling Flow and Heat Transfer in Coiled and Twisted Pipes, Adv. Transport Process., 4(1986), 49-112.
[2] S. Yanase, Y. Kaga and R. Daikai, Laminar flow through a curved rectangular duct over a wide range of the aspect ratio, Fluid Dynamics Research, 31(2002), 151-183.
[3] M. Selmi and K. Namdakumar, Bifurcation Study of the Flow Through rotating Curved Ducts, Physics of Fluids, 11(1999), 2030-2043.

[4] K. Yamamoto, S. Yanase and M. M. Alam, Flow through a Rotating Curved Duct with Square Cross-section, J. Phys. Soc. Japan, 68(1999), 1173-1184.

[5] R. N. Mondal, M. M. Alam and S. Yanase, Numerical prediction of non- isothermal flows through a rotating curved duct with square cross section, Thommasat Int. J. Sci and Tech., 12(3)(2007), 24-43.

[6] R. N. Mondal, and A. K. Datta, Dean-Taylor flow through a rotating curved square duct: The case of negative rotation, Int. J. Appl. Math & Engg. Sci., 4(1)(2010), 65-75**.**

[7] L. Q. Wang and K. C. Cheng, Flow Transitions and combined Free and Forced Convective Heat Transfer in Rotating Curved Channels: the Case of Positive Rotation, Physics of Fluids, 8(1996), 1553-1573.

[8] R. N. Mondal, A. K. Datta and M. K. Uddin, A Bifurcation Study of Laminar Thermal Flow through a Rotating Curved Duct with Square Cross-section, Int. J. Appl. Mech. and Engg., 17(2)(2012), (In Press).

[9] R. N. Mondal, M. S. Uddin, M. S. Islam and M. N. Akhter, Transition to Chaos for Non-isothermal Flows through a Curved Rectangular Duct. Journal of Calcutta Mathematical Society, 8(2)(2013), 103-116.